JOURNAL OF GEOPHYSICAL RESEARCH: ATMOSPHERES, VOL. 118, 9766–9777, doi:10.1002/jgrd.50779, 2013

Decadal changes of Meiyu rainfall around 1991 and its relationship with two types of ENSO

Jian Zhu,[1] Dan-Qing Huang,[2] Yao-Cun Zhang,[2] An-Ning Huang,[2] Xue-Yuan Kuang,[2] and Ying Huang[2]

Received 16 May 2013; revised 22 August 2013; accepted 22 August 2013; published 11 September 2013.

[1] This study investigates Meiyu (June-July) rainfall from 1980 to 2000 over Yangtze-Huaihe River valley (YHRV) and reveals a decadal change around 1991 with a seesaw-like distribution. This decadal change is closely associated with negative phase of preceding winter El Niño–Southern Oscillation (ENSO) Modoki (EM) in the pre-1991 epoch and positive phase of conventional ENSO (CE) in the post-1991 epoch. In response to negative EM (pre-1991 epoch), the source of water vapor is western North Pacific, associated with the eastward retreat of western Pacific subtropical high (WPSH) and the northward shift of East Asian westerly jet (EAWJ). On the other hand, in response to positive CE (post-1991 epoch), water vapor generally comes from the South China Sea, associated with the enhancement and westward advance of the WPSH and southward shift of the EAWJ. Two possible mechanisms are proposed to explain the relationship between preceding winter sea surface temperature (SST) and Meiyu rainfall over YHRV in the two epochs. In the pre-1991 epoch, due to enhanced precipitation, solar radiation decreases, resulting in SST cooling over western North Pacific in Meiyu period. An anomalous anticyclone associated with the SST cooling suppresses precipitation over northern part of YHRV. Meanwhile, an anomalous cyclone accompanied with the anticyclone locates over East China Sea and brings more precipitation to the southern part of YHRV. In the post-1991 epoch, the persistent simultaneous warming in eastern equatorial Pacific and Indian Ocean leads to abundant moisture brought to southern China. Further analysis suggests that the two types of ENSO have asymmetric features with respect to the impact of their positive and negative phases on the seesaw-like Meiyu rainfall, which is closely related with EM La Niña (CE El Niño) in the pre-1991 epoch (post-1991 epoch).

Citation: Zhu, J., D.-Q. Huang, Y.-C. Zhang, A.-N. Huang, X.-Y. Kuang, and Y. Huang (2013), Decadal changes of Meiyu rainfall around 1991 and its relationship with two types of ENSO, *J. Geophys. Res. Atmos.*, *118*, 9766–9777, doi:10.1002/jgrd.50779.

1. Introduction

[2] Rainy season or rainband in an East Asia summer monsoon (EASM) season is called the Baiu in Japan, the Meiyu in China, and the Changma in Korea (hereafter referred to as Meiyu). During Meiyu season, the rainband stagnates over the Yangtze-Huai River valley (YHRV, 110°E–122°E, 28°N–34°N), with its eastern edge passing through the Japan Islands. The main Meiyu season in China starts from late June and ends in early July. In Meiyu period, heavy precipitation events occur frequently and lead to natural disasters. Therefore, understanding the variations of Meiyu over YHRV is important.

[3] East Asian climate has experienced an interdecadal scale transition since the late 1970s [*Wang*, 2001; *Wu and Wang*, 2002; *Yu et al.*, 2004; *Xin et al.*, 2006; *Yu and Zhou*, 2007; *Zhou et al.*, 2009a,b; *Zhou and Huang*, 2010]. This transition is also evident in Meiyu [*Hu*, 1997; *Xu*, 2001; *Gong and Ho*, 2002; *Ye and Lu*, 2011; *Ding*, 1992]. Since late 1970s, the rainband shifted southward over China, with excessive rainfall along the middle and lower reaches of YHRV, and deficient rainfall in northern China [e.g., *Hu et al.*, 2003; *Yu and Zhou*, 2007]. Recently, the latest changing point of Meiyu systems around 2000 has been revealed [*Liang and He*, 2008; *Si et al.*, 2009; *Huang et al.*, 2011], e.g., rainy belt, the persistent Meiyu rainfall, and the spatial distribution, the onset and withdraw of Meiyu period. Moreover, some studies indicated that the decadal shift of summer rainfall and large-scale circulation over East Asia was around the 1990s. *Ding et al*. [2008] found that the summer rainfall in Eastern China demonstrated a decadal shift in the beginning of 1990s. *Yim et al*. [2008] indicated a decadal change in summer monsoon system and western North Pacific around 1992. *Kajikawa and Wang* [2012] detected a significant advance in the onset dates of the South China Sea summer monsoon around 1993/1994. *Yim et al*. [2013] indicated that the interannual variation of the May-June precipitation in EASM and the processes controlling the variation have been changed abruptly around the mid-1990s. Thus far, most efforts undertaken have been focused on the

[1]State Key Laboratory of Hydrology-Water Resources and Hydraulic Engineering, Hohai University, Nanjing, China.
[2]School of Atmospheric Sciences, Nanjing University, Nanjing, China.

Corresponding author: D. Huang, School of Atmospheric Sciences, Nanjing University, Nanjing Jiangsu 210093, China. (huangdq@nju.edu.cn)

2169-897X/13/10.1002/jgrd.50779

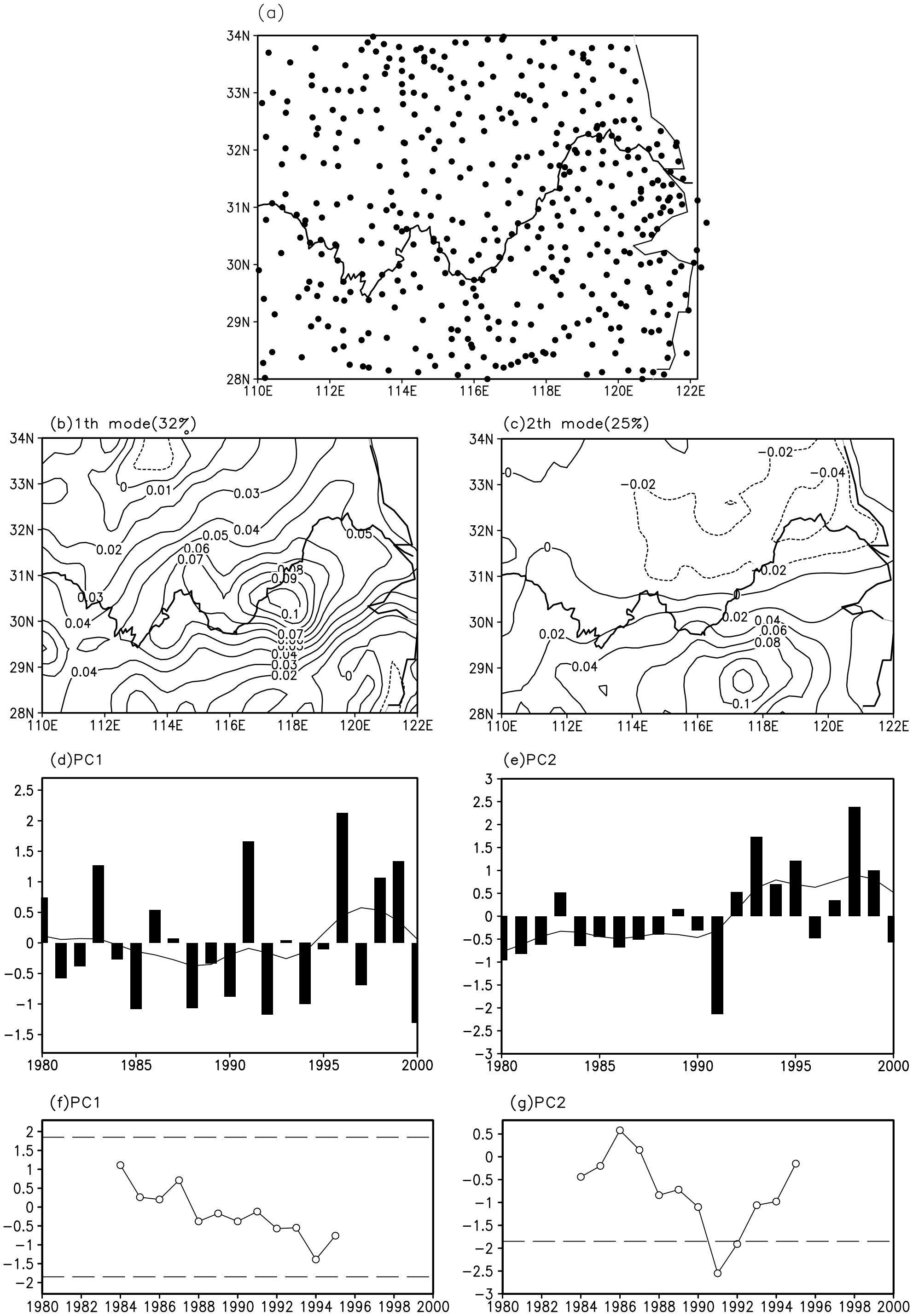

Figure 1. (a) Location of 422 stations in YHRV; summer rainfall EOF spatial pattern, (b) EOF1 and (c) EOF2; and their normalized principle components, (d) PC1 and (e) PC2 during 1980–2000; the running *t* test of (f) PC1 and (g) PC2 with a 5 year running window. The line in Figures 1d and 1e indicate the 11-running average. The dashed lines in Figures 1f and 1g indicate the above 90% confidence level of the running *t* test.

decadal scale transition around the late 1970s and 2000 of Meiyu over YHRV. Moreover, some studies indicated a decadal shift in 1990s for summer rainfall and the associated large-scale circulations over East Asia. However, whether Meiyu has a decadal change in the 1990s during period from 1980 to 2000 is still not clear.

[4] The oceanic anomaly is an important factor for the variations of EASM, especially for the interdecadal shift around late-1970s. For example, the weakening of EASM since late-1970s is partially due to the warming in Indian Ocean, far western Pacific, and the tropical central-eastern Pacific [*Li et al.*, 2010]. *Hu* [1997] suggested that the change of sea

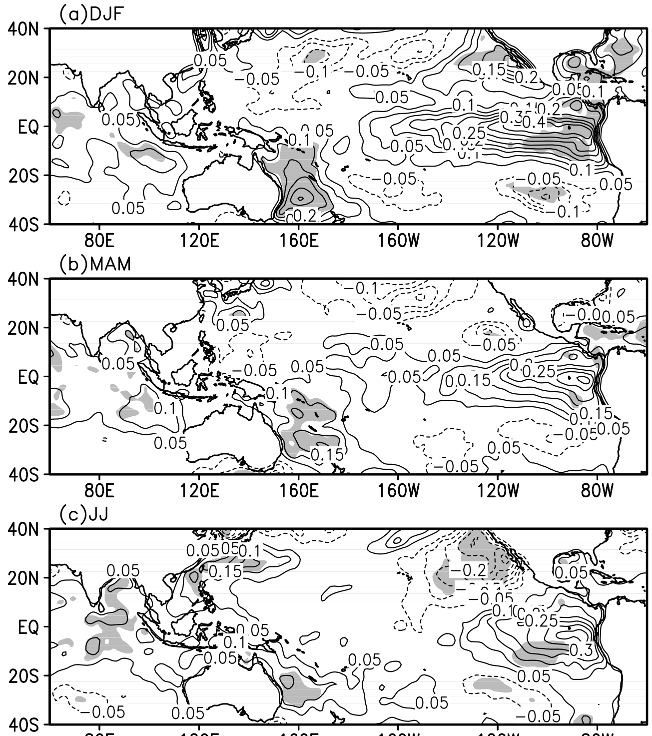

Figure 2. Regression of preceding (a) DJF, (b) MAM, and (c) simultaneous JJ SST with respect to PC1 for the period of 1980–2000. The shaded areas denotes regions with correlation significance at the 95% confidence level (unit: °C).

surface temperature (SST) over the tropical Indian Ocean and tropical western Pacific occurring around 1976–1979 was a potential reason for the interdecadal change of EASM. *Wu and Wang* [2002] noted that the summer rainfall anomaly along the middle to lower reaches of the Yellow River valley was caused by the changes in the EASM circulation anomaly related with El Niño–Southern Oscillation (ENSO), which was attributed to the changes in the location and intensity of anomalous convection over the western North Pacific and India. As mentioned, some robust SST regions have been revealed, e.g., South China Sea [*Wan et al*., 2008; *Zhou*, 2011], eastern equatorial Pacific [*Wang et al*., 2000; *Wu and Wang*, 2002; *Wu et al*., 2005; *Zhu et al*., 2010; *Ye and Lu*, 2011], and Indian Ocean [*Huang et al*., 2010; *Yang et al*., 2007; *Li et al*., 2008]. On decadal transition around 1990s, the dominant SST patterns are still unknown in despite of the climate importance.

[5] Therefore, the objective of this study is to investigate the decadal change of Meiyu in 1980–2000 and the associated SST variations. Specifically, we try to answer the following questions:

[6] 1. Whether there is a decadal change in 1980–2000? If so, what are the dominant SST variations associated with?

[7] 2. What are the possible linkages between SST activities and the decadal variation of Meiyu?

[8] The rest of the paper is arranged as follows: Section 2 describes the data sets and methods used in this study. In section 3, the decadal variation of Meiyu rainfall over YHRV in 1980–2000 and the relationship with preceding winter (December-January-February, DJF) SST are investigated. Section 4 shows the three-dimensional circulations associated with the dominant SST activities. Section 5 discusses the possible mechanism linking preceding winter SST and Meiyu rainfall over YHRV in the two epochs. The conclusion and discussion are given in section 6.

2. Data and Methodology

[9] Several data sources during period from 1980 to 2000 are used in this study: (1) daily precipitation data (June and July) of 422 stations in YHRV (Figure 1a) provided by China Meteorological Administration, (2) global monthly SST data from the Hadley Center with a resolution of 1° × 1° [*Rayner et al*., 2003], (3) global monthly precipitation data from Global Precipitation Climatology Project Version 2.2 [*Huffman et al*., 2011], and (4) monthly atmospheric data from the National Centers for Environmental Prediction-National Center for Atmospheric Research reanalysis [*Kalnay et al*., 1996].

[10] The statistic techniques of empirical orthogonal function (EOF) analysis, running *t* test, and partial correlation are used in this study. Partial correlation (regression) technique is used to show exclusive relationship between two variables while excluding influence arising from another independent variable [*Behera and Yamagata*, 2003]. For example, the partial correlation (regression) between *A* and *B*, while excluding the relation arrived because of the correlation between *B* and *C*, is defined as follows,

$$r_{AB,C} = \frac{r_{AB} - r_{AC}r_{BC}}{\sqrt{(1 - r_{AC}^2)}\sqrt{(1 - r_{BC}^2)}} \quad (1)$$

where r_{AB}, r_{AC}, and r_{BC} are the correlations between *A* and *B*, *A* and *C*, and *B* and *C*, respectively. Statistical significance of the correlation coefficients is evaluated by a two-tailed "*t* test."

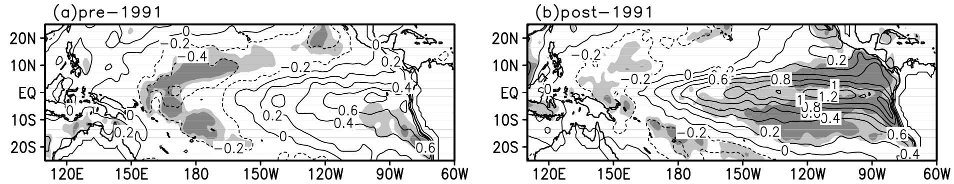

Figure 3. Regression of preceding DJF SST with respect to PC2 for the (a) pre-1991 epoch and (b) post-1991 epoch. The light (dark) shaded areas denotes regions with correlation significance at the 95% (99%) confidence level (unit: °C).

Table 1. Positive and Negative Years Based on Principle Component for EOF2 in 1980–1991 and 1992–2000

	1980–1991	1992–2000
Positive years	1983, 1989	1993, 1998
Negative years	1980, 1991	1996, 2000

3. Decadal Changes of Meiyu Rainfall Over YHRV and its Relationship With Preceding Winter SST

[11] The EOF analysis is performed to detect the decadal change of Meiyu (June-July, JJ) rainfall over YHRV. Figure 1 shows the spatial patterns of the first two leading EOF modes (EOF1 and EOF2) and their corresponding normalized principal components (denoted as PC1 and PC2, respectively). The first and second modes explain 32% and 25% of the total variance, respectively, and are clearly separated from the higher modes [*North et al.*, 1982].

[12] The EOF1 (Figure 1b) shows a monopole pattern over the entire YHRV, and the EOF2 (Figure 1c) exhibits a seesaw-like pattern divided by the Yangtze River. As shown in Figures 1d and 1f, PC1 is dominated by interannual variation without significant decadal shift. However, in Figures 1e and 1g, PC2 indicates that the Meiyu rainfall over YHRV exhibits a significant decadal change around 1991. Combined with spatial pattern of EOF2 (Figure 1c), before 1991, negative phase implies a real rainfall pattern of "southern drought northern flood" over YHRV. After 1991, the phase turns to positive, implying a "southern flood northern drought" rainfall pattern. Previous studies indicated that interannual variation of Meiyu rainfall was closely related to SST variations [*Huang and Wu*, 1989; *Zhao and Qian*, 2009]. As shown in Figure 2, the regression of SST against PC1 indicates that the positive SST anomalies exist over the eastern coast of Australia in the preceding winter and spring, while over South China Sea in the simultaneous Meiyu period. This is consistent with the results of *Ma et al.* [2012]. However, for decadal variation shown in PC2, whether the SST variations leading Meiyu rainfall over YHRV have changed is still not clear. To solve this, the regression of preceding winter SST against PC2 is performed for the pre-1991 epoch and the post-1991 epoch, respectively. In the pre-1991 epoch (Figure 3a), the dominant areas with significant correlation are distributed in the following places: the tropical central Pacific with remarkable tongue-like negative correlation and northwestern coast of Australia with a significant positive correlation. This is similar to the ENSO Modoki (EM) pattern [*Ashok et al.*, 2007; *Weng et al.*, 2007], which is defined as the central equatorial Pacific being warmer while the flanked areas on both sides along the eastern equatorial Pacific and western Pacific (primarily on warm pool) being colder. However, in the post-1991 epoch (Figure 3b), the significant positive correlation exists over the central and eastern equatorial Pacific, which is commonly recognized as conventional ENSO (CE). It indicates the mature phase (in winter) of the El Niño event has considerable relationship with the Meiyu rainfall over YHRV in the post-1991 epoch. To confirm these relationships in the two epochs, composite analysis is used to check the SST variation. The corresponding principle component for EOF2 is separated into two parts for the pre-1991 and post-1991 epochs. Typical positive (negative) years are chosen separately for the two epochs with standard deviation of the principle component exceeding +1(−1) (as shown in Table 1). Figure 4 shows the preceding winter SST differences between the positive and negative years in the two epochs. Apparently, in the pre-1991 epoch, the SST variation is characterized by a zonal triple pattern as "+/−/+" anomalies over "eastern/central/western" part of tropical region [*Ashok et al.*, 2007], which can be identified as EM La Niña. In the post-1991 epoch, the SST variation resembles the traditional El Niño pattern with strong warming over eastern tropical Pacific [*Rasmusson and Carpenter*, 1982]. It indicates that the key preceding winter SST regions related with Meiyu rainfall over YHRV have changed in different periods. The preceding winter SST signal is negative EM (positive CE) in the pre-1991 epoch (post-1991 epoch). Moreover, the SST signals in spring and summer show similar decadal changes but with less strength (figure omitted). The mature phase of ENSO often occurs in boreal winter and is usually accompanied by a weaker than normal winter monsoon along the East Asian coast [*Zhang et al.*, 1996; *Tomita and Yasunari*, 1996; *Ji et al.*, 1997; *Wang et al.*, 2000; *Wu et al.*, 2009]. The ocean warming persists through the following spring and summer and exerts its climatic influence on East Asia after ENSO, like a discharging capacitor [*Xie et al.*, 2010; *Wu et al.*, 2009]. Thus, the preceding winter SST variations can be considered as a predictor of Meiyu rainfall. And we focus on the relationship of preceding winter SST variations with Meiyu rainfall and its possible mechanisms in the following analysis.

[13] Two indices are calculated to identify the SST variations during different periods. The EM index is defined by *Ashok et al.* [2007], as follows,

$$\text{EM index} = [\text{SSTA}]_A - 0.5 \times [\text{SSTA}]_B - 0.5 \times [\text{SSTA}]_C \quad (2)$$

[14] The square bracket in equation 2 represents the SSTA (sea surface temperature anomaly) averaged over a central region (A: 165°E–140°W, 10°S–10°N), an eastern region

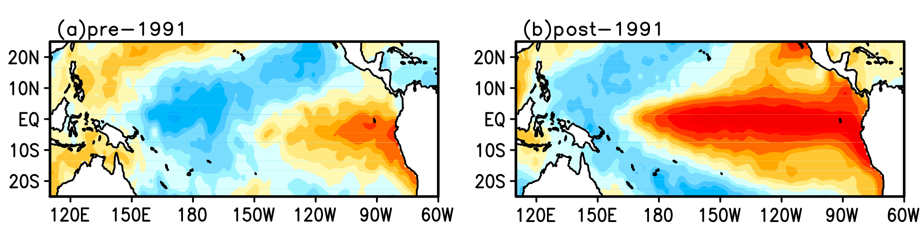

Figure 4. Composites of preceding DJF SST differences between typical positive and negative years in the (a) pre-1991 epoch and (b) post-1991 epoch (unit: °C).

Table 2. Partial Correlation Coefficient Between the PC2 and EM Index (Niño3) in 1980–1991 (1992–2000)[a]

	1980–1991	1992–2000	1980–2000
PC2-EM index	**−0.80**	0.16	−0.38
PC2-Niño3	0.60	**0.74**	0.51

[a]The values given in bold are significant at 95% confidence level.

(B: 110°W–70°W, 15°S–5°N), and a western region (C: 125°E–145°E, 10°S–5°N), respectively. The index is available at http://www.jamstec.go.jp/frcgc/research/d1/iod/modoki_home.html.en. The Niño3, identifying CE, is available at http://www.cpc.noaa.gov/data/indices/. Although the correlation between monthly EM index and Niño3 is insignificant ($R = 0.2$), the correlation in winter is much higher ($R = 0.38$ for pre-1991 and $R = 0.5$ for post-1991), exceeding the 95% significant confidence level. Thus, partial correlation is used to show exclusive relationship between EM (CE) and PC2 while excluding influence arising from CE (EM). The partial correlation coefficients during 1980–1991 and 1992–2000 are shown in Table 2. It indicates a strong negative (positive) relationship between EM (CE) and Meiyu rainfall in the pre-1991 epoch (post-1991 epoch).

4. Three-Dimensional Circulations Associated With EM and CE in the Two Epochs

[15] To understand the variability of Meiyu rainfall associated with different SST anomalies over the related key regions, the regional and background atmospheric circulations are analyzed. Since the correlation between EM index (Niño3) and PC2 in the pre-1991 epoch (in the post-1991 epoch) is negative (positive), in order to compare to the real rainfall pattern over YHRV as shown in the description of EOF2, negative EM index and positive Niño3 are used to investigate the relationship between the SST variations and the atmospheric circulations by partial regression.

[16] Water vapor content is one of the major factors directly affecting the summer rainfall over Eastern China [*Zhou and Yu*, 2005]. Figure 5 shows the vertically integrated moisture transport (VIMT) from 1000 to 300 hPa obtained by the partial regressions with respect to the preceding winter negative EM and positive CE in the two epochs. In response to negative EM (1980–1991) (Figure 5a), a significant westward VIMT exists over the western North Pacific (20°N–40°N, 115°E–160°E). While in response to positive CE (1992–2000) (Figure 5b), a significant northeastward VIMT locates over southern China. This suggests that the sources of water vapor for Meiyu in response to negative EM (1980–1991) and positive CE (1992–2000) are different.

[17] The vertical atmospheric circulation is examined to understand the impacts of negative EM and positive CE on Meiyu rainfall. In response to negative EM (1980–1991), since water vapor comes from western North Pacific but rainfall is south–north seesaw-like pattern, Figures 6a and 6c show partial regressions of longitude-height cross sections of vertical circulations averaged over 28°N–31°N and 31°N–34°N, respectively. In Figure 6a, significant descent motion covers southern part (28°N–31°N) of YHRV, and decreased humidity occupies entire vertical levels. In Figure 6c, for the northern part (31°N–34°N) of YHRV, ascent motion with dominantly increased humidity locates over eastern area while descent motion locates over the western area. Combination of these vertical circulations favors the "southern drought northern flood" pattern of Meiyu rainfall. In response to positive CE (1992–2000), since VIMT direction is parallel to the rainfall from south to north, Figure 6b shows partial regressions of latitude-height cross sections of vertical circulations averaged over 110°E–112°E. Ascent/descent motion with abundant/insufficient water vapor over the southern/northern part of YHRV results in the "southern flood northern drought" pattern for Meiyu rainfall in the post-1991 epoch.

[18] As well known, the Meiyu rainfall is associated with large-scale atmospheric circulations such as the western Pacific subtropical high (WPSH), the East Asian subtropical westerly jet (EAWJ), and other atmospheric circulations [*Akiyama*, 1975; *Tao and Chen*, 1987; *Zhang et al.*, 2006]. Figure 7 shows the anomalies of geopotential height at 500 hPa obtained by partial regressions with respect to the preceding winter negative EM and positive CE in the two epochs. In response to negative EM (1980–1991) (Figures 7a and 7c), prominent feature shows a significant negative anomaly located over the western part of WPSH (generally considered as regions surrounded by 5880-line), indicating anomalous eastward retreat of the WPSH, which may result in decreased precipitation over southern China. *Feng et al.* [2010a] also revealed the western North Pacific anticyclone shifts the ridge of WPSH westward in summer for the case of El Niño years. In response to positive CE (1992–2000) (Figures 7b and 7d), significant positive anomaly covers the WPSH region and its western area, indicating the WPSH strengthens and advances westward. This may result in the anomalous southwestern VIMT shown in Figure 5b, leading to the enhanced moisture supply to the southern China.

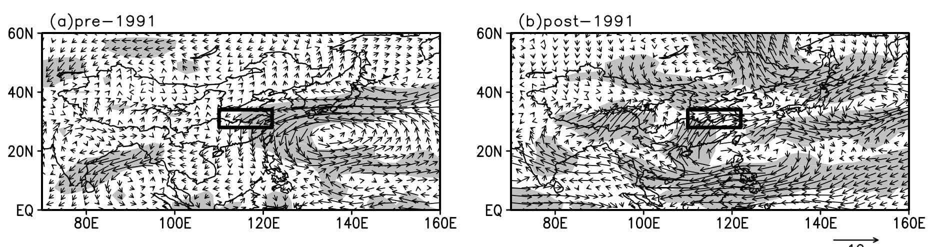

Figure 5. Partial regressions of June-July (JJ) VIMT from 1000 to 300 hPa (vector, unit: kg·(m s)$^{-1}$) with respect to normalized DJF (a) negative EM index for the pre-1991 epoch and (b) positive Niño3 for the post-1991 epoch. The regions over 95% significant confidence levels are shaded. The box indicates the location of YHRV.

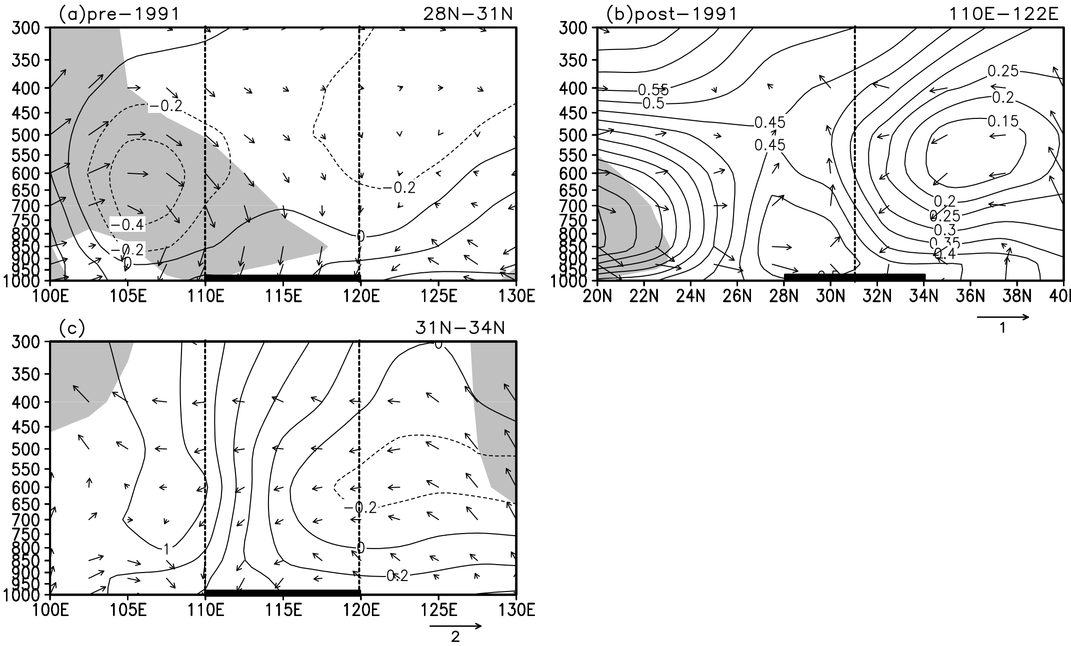

Figure 6. Longitude-height cross sections averaged over (a) 28°N–31°N, (c) 31°N–34°N, and latitude-height cross sections averaged over (b) 110°E–122°E of the partial regression of JJ vertical motion (unit: m/s, vector) and specific humidity (unit: $\times 10^{-3}$ g/kg, solid line) with respect to normalized DJF negative EM index for the pre-1991 epoch (Figures 6a and 6c) and positive Niño3 for the post-1991 epoch (Figure 6b). The shaded regions denote with the correlation of vertical velocity significant at the 95% confidence level. The black area on the *x* coordinate indicates the region of YHRV.

[19] Figure 8 shows the anomalies of zonal wind at 200 hPa obtained from partial regressions with respect to the preceding winter negative EM and positive CE anomalies in the two epochs. In response to negative EM (Figure 8a), significant "−/+" dipole anomalies are located over the northern and southern area of the axis of EAWJ, indicating the enhancement and northward shift of EAWJ over continent, which may increase precipitation over the northern part of YHRV [*Du et al.*, 2009]. In response to positive CE (Figure 8b), the positive anomalies are located over the southern part of the

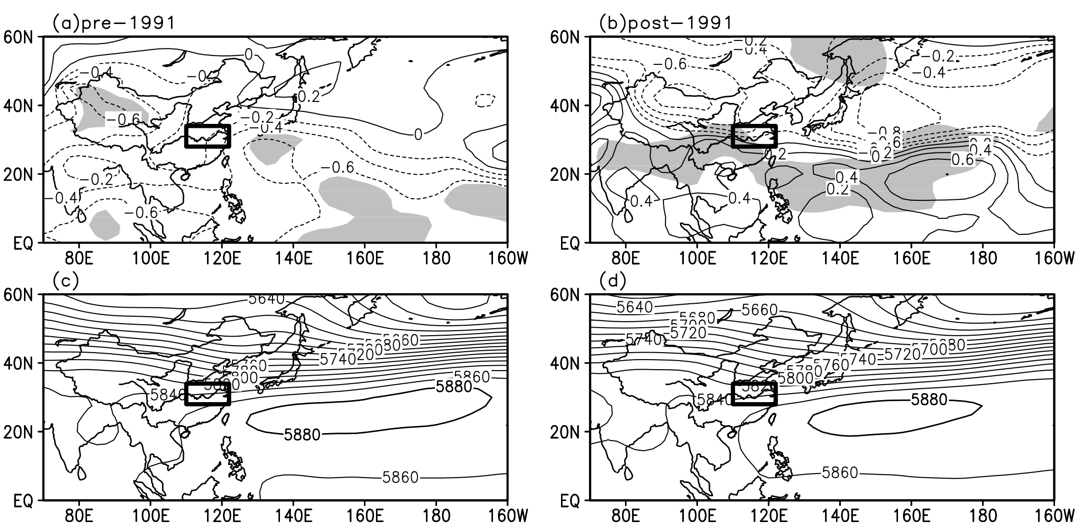

Figure 7. Partial regressions of June-July (JJ) geopotential height at 500 hPa (unit: gpm) with respect to normalized DJF (a) negative EM index for the period of in the pre-1991 epoch and (b) positive Niño3 in the post-1991 epoch. The climatology geopotential height at 500 hPa (unit: gpm) (c) in the pre-1991 epoch and (d) in the post-1991 epoch. The box indicates the location of YHRV. The shaded regions denote with the correlation significance at the 95% confidence level.

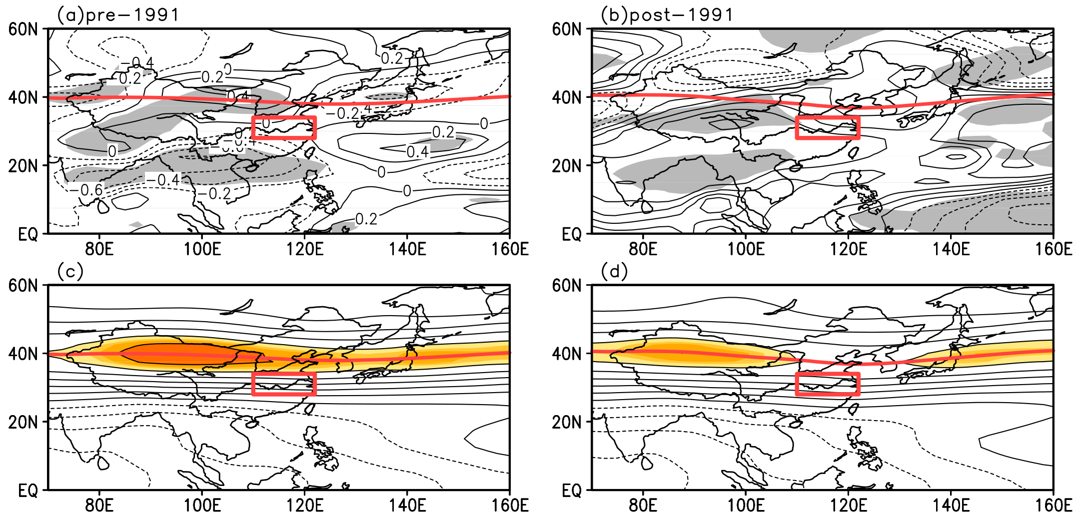

Figure 8. Same as Figure 7, but for zonal winds at 200 hPa (unit: m/s). (a and b) The red thick solid line indicate the EAWJ axis in the pre-1991 epoch and the post-1991 epoch, respectively. The box indicates the location of YHRV. In Figures 8a and 8b, the shaded regions denote with the correlation significance at the 95% confidence level. (c and d) The shading denotes the regions with zonal winds exceeding 30 m/s.

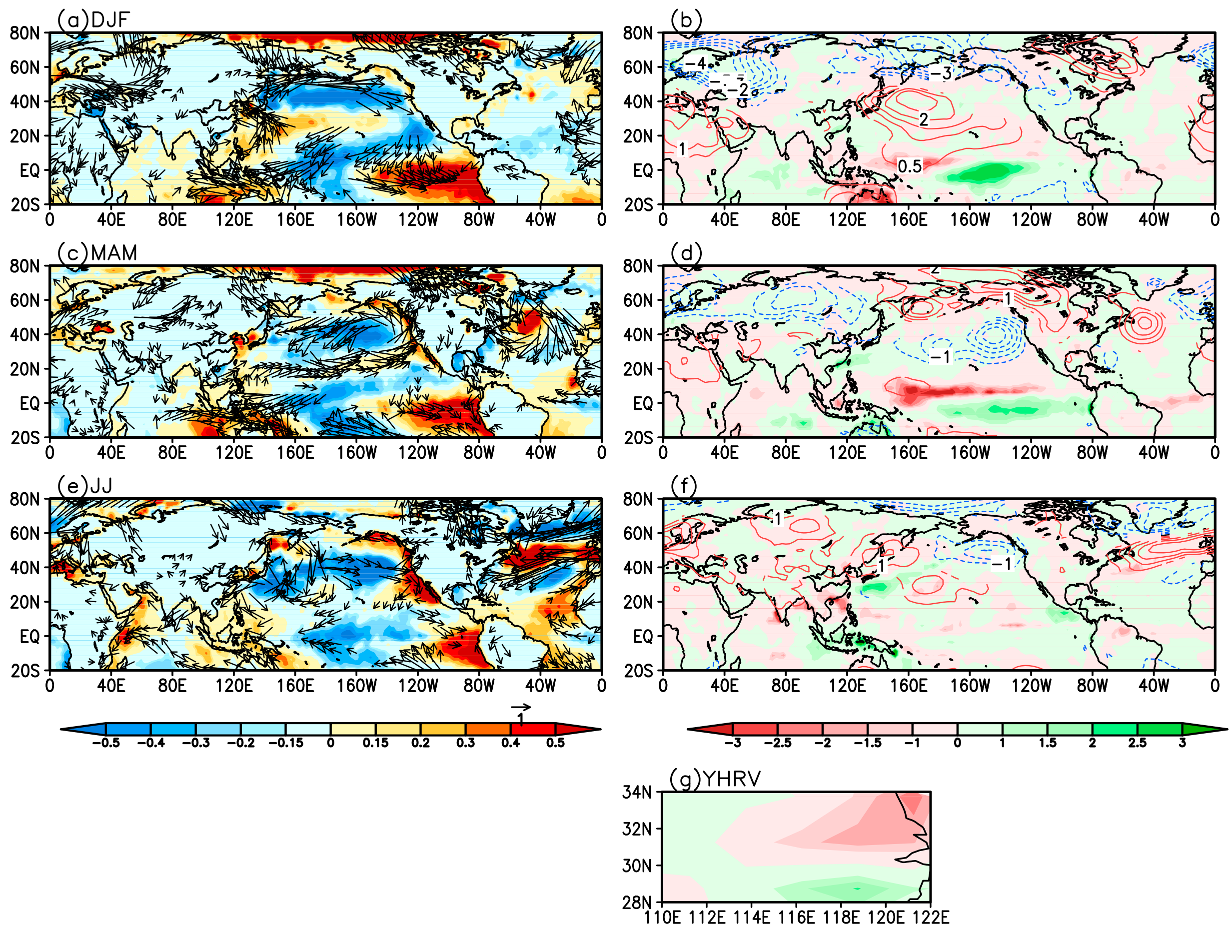

Figure 9. The regressed SST (shaded), winds (vector) at 925 hPa, precipitation (shaded), SLP (contour) anomalies during (a and b) DJF, (c and d) MAM, (e and f) JJ, and the JJ precipitation anomalies (shaded) over (g) YHRV with respect to PC2 in the pre-1991 epoch. The wind vectors and SLP that are significant above the 95% confidence level by Student's *t* test.

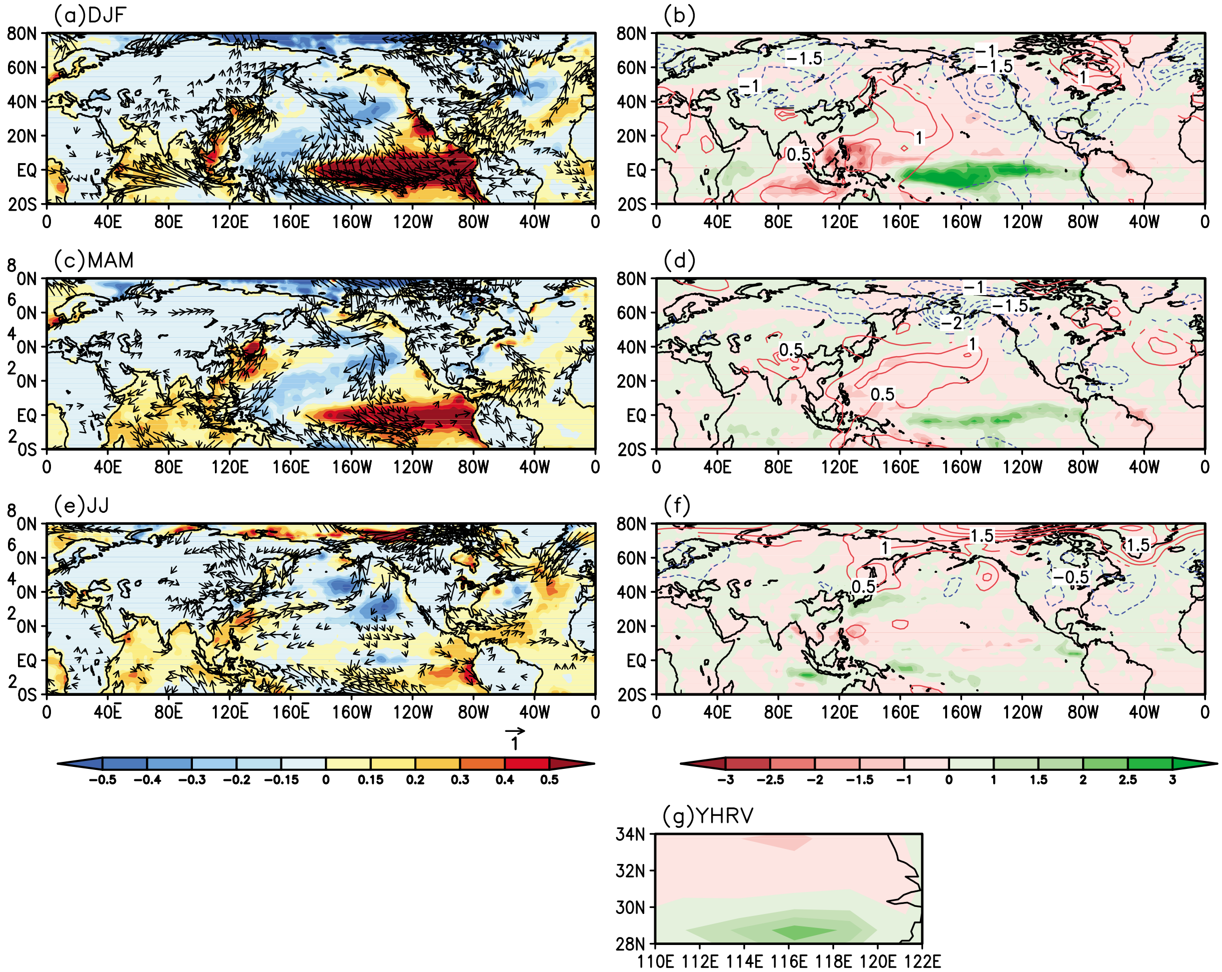

Figure 10. Same as Figure 9 except for the post-1991 epoch.

axis of EAWJ, indicating the southward movement of EAWJ, which results in the large precipitation center moving southward.

5. Possible Mechanisms Linking Preceding Winter SST and Meiyu Rainfall Over YHRV in the Two Epochs

[20] Above all, there is a close relationship between the preceding winter SST and Meiyu rainfall over YHRV. Then, how does the atmospheric circulation in Meiyu period establish in the two epochs? Most studies explained the relationship between preceding winter SST and summer rainfall over China in the aspect of the outgoing longwave radiation [*Yuan et al.*, 2012], persistent SST anomalies from winter to summer [*Feng et al.*, 2010b; *Chen et al.*, 2013], or the central Pacific warming-induced Philippine Sea anticyclone [*Yim et al.*, 2013]. To shed light on this, we investigate the atmospheric circulations and precipitation anomalies with seasonal interval extending in preceding DJF, MAM (March-April-May), and simultaneous JJ.

[21] Figure 9 shows the regressed SST, 925 hPa winds, precipitation, and sea level pressure (SLP) anomalies with respect to PC2 in 1980–1991. In the pre-1991 epoch, associated with the SST cooling over most part of North Pacific (Figure 9a), positive SLP anomaly over North Pacific lead to an anomalous anticyclone (Figure 9b), resulting in suppressed precipitation (Figure 9b). At the same time, associated with significant warming over East China Sea (Figure 9a), a cyclone anomaly benefits the enhanced precipitation. This enhanced precipitation will decrease the downward solar radiation (figures not shown) and results in less warming over East China Sea in the following MAM (Figure 9c). Meanwhile, accompanied with the negative SLP anomalies over northern North Pacific (Figure 9d), an anomalous cyclone forms (Figure 9c), resulting in enhanced precipitation, especially over the western part (Figure 9d). Consequently, SST cooling intensifies and a western cooling center forms over western North Pacific in JJ (Figure 9e). The surface cooling leads to an anticyclone associated with the increased SLP (Figures 9e and 9f), resulting in decreased precipitation over the northern part of YHRV (Figure 9g). Accompanied with the anticyclone anomaly, an anomalous cyclone occupies East China Sea with decreased SLP (Figures 9e and 9f), resulting in increased precipitation over the southern part of YHRV (Figure 9g).

[22] In the post-1991 epoch, there is an obvious warming over eastern equatorial Pacific with abundant precipitation anomalies in DJF, MAM, and JJ. Meanwhile, the warming over Indian Ocean lasts from DJF to JJ (Figures 10a, 10c, and 10e). This is in good agreement with the findings of *Xie et al.* [2009] and *Wu et al.* [2009, 2010b], which indicated that the Indian Ocean warming in response to the atmospheric

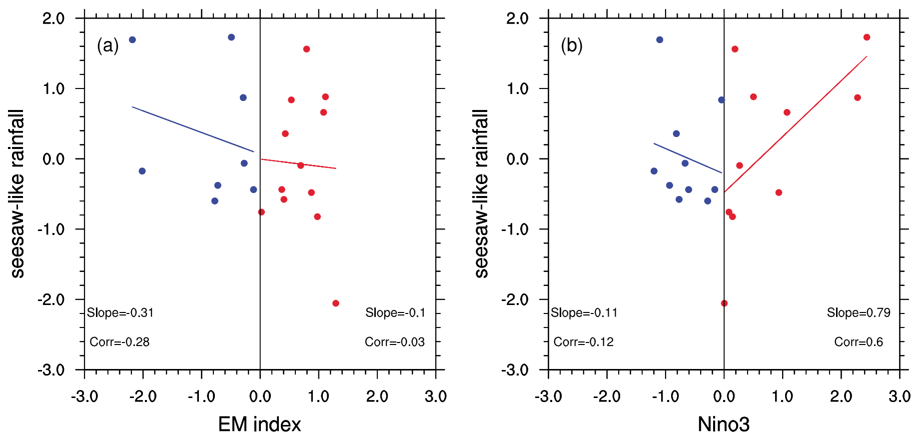

Figure 11. Normalized JJ seesaw-like rainfall anomaly over YHRV plotted against (a) EM index and (b) Niño3 in the period of 1980–2000. Lines of best fit for positive and negative EM index and Niño3 values, and the correlation coefficients (Corr) and regression coefficients (Slope) are also given.

teleconnection forced by an El Niño event was similar to a battery charging a capacitor. Additionally, the SST cooling over western North Pacific between the two warming areas is also important and has been demonstrated by numerical modeling experiments in *Wu et al.* [2010b], which demonstrated that the colder SST in western North Pacific drives the western Pacific atmospheric circulation in early summer. This suggests that more water vapor is transported to southern China while a positive SLP anomaly covers the northern China, which may lead to the increased (decreased) rainfall along 20°N–31°N (31°N–34°N) (Figure 10g).

6. Conclusions and Discussions

[23] This study reveals an obvious decadal change (EOF2) in Meiyu rainfall over YHRV around 1991 with a seesaw-like variation pattern. The regressions show that the rainfall pattern is associated with EM La Niña (CE El Niño) in 1980–1991 (1992–2000).

[24] The source of water vapor is western North Pacific in respective to negative EM, associated with the western Pacific subtropical high (WPSH) retreats eastward and the East Asian westerly jet (EAWJ) exhibits a northward shift. However, in respective to positive CE, water vapor generally comes from the South China Sea, which is associated by the enhancement and westward advancing of the WPSH and southward shift of the EAWJ. Meanwhile, the vertical structures of winds and moisture benefit the seesaw-like pattern over YHRV. In the pre-1991 epoch, the significant ascending motion and increased moisture occur over the northern part of YHRV, while the opposite features occur in the southern part, vice versa in the post-1991 epoch.

[25] We propose two possible mechanisms to explain how preceding winter SST affects Meiyu in the two epochs. In the pre-1991 epoch, the enhanced precipitation over East China Sea decreases the downward solar radiation and results in SST cooling in MAM. An anomalous cyclone forms associated with the negative SLP anomalies over North Pacific, resulting in enhanced precipitation, especially over the western part. Consequently, western cooling center forms over western North Pacific in JJ, leading to an anticyclone associated with the increased SLP. Accompanied with this, an anomalous cyclone with decreased SLP covers East China Sea. These features favor the same seesaw-like rainfall pattern as the EOF2 spatial distribution. In the post-1991 epoch, the simultaneous warming is indicated over eastern equatorial Pacific and Indian Ocean and cooling exits over the western North Pacific. Correspondingly, more abundant water vapor has been transported to southern China while a positive SLP anomaly covers the northern China, which may also leads to the seesaw-like rainfall pattern over YHRV.

[26] Recent studies revealed the new variant of the El Niño phenomenon, EM El Niño, which occurs frequently after 1990s [*Yeh et al.*, 2009]. However, our study shows a close relationship between the Meiyu rainfall and EM before 1991. Why is there a close relationship indicated in the earlier period? Although the EM El Niño received more attention mainly after 1990s, some significant EM La Niña years can still be picked out by the EM index before 1991 (e.g. 1983, 1989) [*Karori et al.*, 2013; *Ashok et al.*, 2007]. Moreover, many studies indicated that the CE El Niño showed significant changes in location although the La Niña was almost unchanged [*Kug et al.*, 2009; *Ren and Jin*, 2011]. In the typical El Niño of 1997–1998 [*McPhaden*, 1999; *Picaut et al.*, 2002], the Yangtze River Valley suffered a severe flood in summer. Thus, the significant relationship between Meiyu rainfall and CE in the post-1991 epoch may be linked with the El Niño events, which suggests possible asymmetric influence exists in El Niño and La Niña on Meiyu rainfall in the decadal changes. Previous studies indicated that the asymmetry in atmospheric circulation anomalies over western North Pacific and eastern Asia is caused by the asymmetric SSTA pattern in the tropical Pacific during the positive and negative phase of both two types of ENSO events [e.g., *Hoerling et al.*, 1997; *Cai et al.*, 2010; *Wu et al.*, 2010a; *Weng et al.*, 2011]. Additionally, the SST-forced teleconnection has changed worldwide [*Hartmann and Wendler*, 2005; *Rodriguez-Fonseca et al.*, 2010]. More recently, *Karori et al.* [2013] indicated that the relationship between rainfall over the YHRV and the EM La Niña is positive and significant, whereas the relationship between the rainfall and the EM El Niño is not. In the case of the CE, its positive phase has a positive influence, while there is no significant relationship with the negative phase.

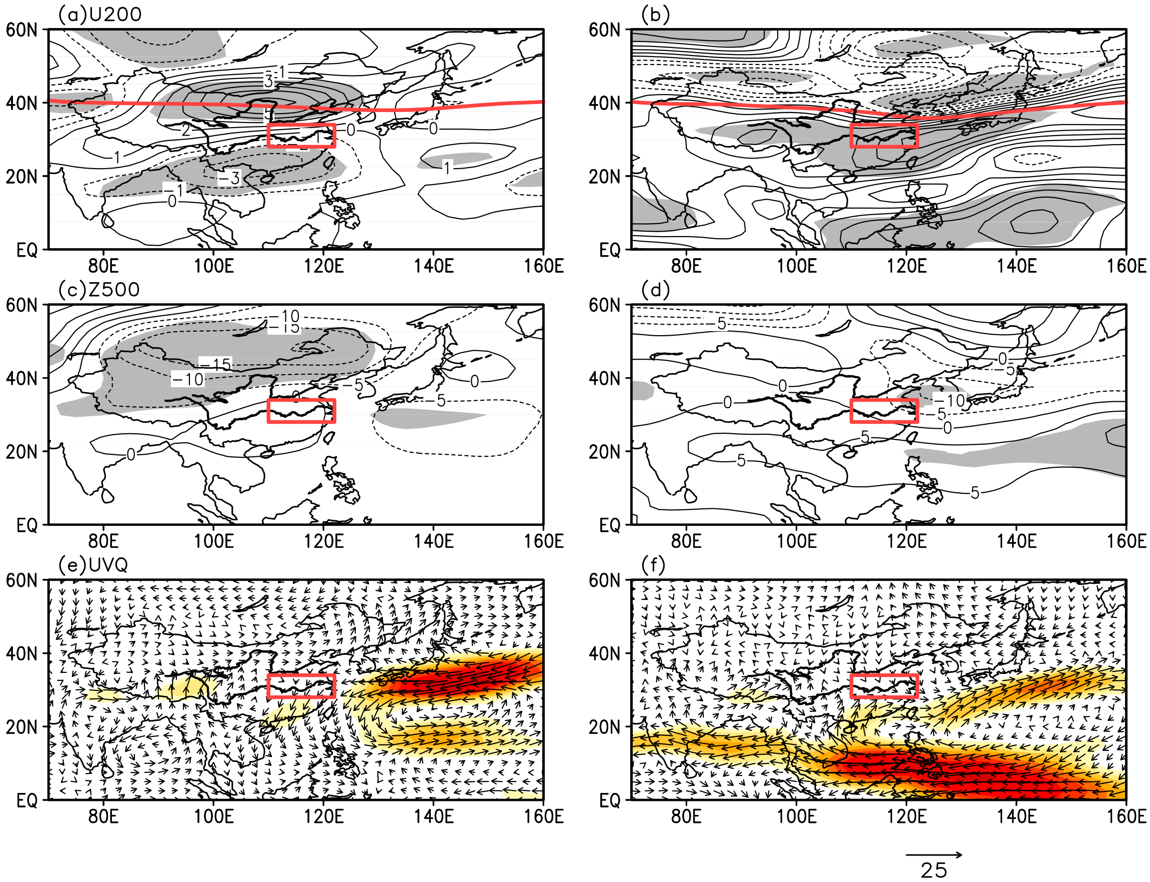

Figure 12. Composites of JJ zonal winds (a and b) at 200 hPa (unit: m/s), geopotential height (c and d) at 500 hPa (unit: gpm), (e and f) VIMT (kg (m s)$^{-1}$) in EM La Niña events in the pre-1991 epoch (Figures 12a, 12c, and 12e) and CE El Niño events in the post-1991 epoch (Figures 12b, 12d, and 12f). The box indicates the location of YHRV. In Figures 12a–12d, the shaded region denote with the correlation significance at the 95% confidence level. In Figures 12a and 12b, the thick solid line indicate the EAWJ axis in the pre-1991 epoch and the post-1991 epoch, respectively. In Figures 12e and 12f, the shaded regions denote the mold of vertically integrated vapor flux from surface to 300 hPa above 6 kg (m s)$^{-1}$.

In contrast, this is opposite for the rainfall over South China. This maybe a possible explanation for the close relationship indicated between EM La Niño and Meiyu rainfall over YHRV in the pre-1991 epoch. To reveal the asymmetry of the relationship, we calculate lines of best fit for the positive and negative phases of the EM and CE. The difference of the regional-averaged Meiyu rainfall between south (28°N–31°N) and north (31°N–34°N) is used to identify the seesaw-like rainfall. Figure 11 shows scatter plots of the normalized seesaw-like rainfall anomaly against EM index and Niño3. The correlation coefficient of the seesaw-like rainfall over YHRV with positive Niño3 is 0.6, and that with the positive EM index is −0.03. The correlation of the seesaw-like rainfall with the negative EM index and Niño3 is −0.28 and −0.12, respectively. There is a significant positive relationship between the seesaw-like rainfall and CE, while it is a weak negative relationship between the seesaw-like rainfall and EM. Similar results are indicated by *Karori et al.* [2013]. Furthermore, composite analysis is used to confirm these findings. Compositions are obtained for the years in which the EM index and Niño3 exceed ±0.5 standard deviation. Following the criteria, significant EM La Niña events during boreal winter in the pre-1991 epoch occurred in 1983–1984, 1984–1985,1985–1986, 1988–1989, while typical El Niño CE events occurred in 1993–1994, 1994–1995, and 1997–1998 in the post-1991 epoch, and the monthly means from June and July of each year are used to calculate the composite mean anomalies. In the case of EM La Niña events, significant "+ −" anomalies of zonal winds at 200 hPa are located over the northern and southern part of EAWJ core (Figure 12a). This favors the northward movement of the EAWJ and results in the increasing precipitation over northern regions. For the geopotential height at 500 hPa, significant decreasing anomalies cover northwestern Pacific (130°E–160°E, 20°N–35°N, Figure 12c), which leads to eastward retreat of the WPSH, resulting in decreased precipitation over southern part of YHRV. This is also in agreement with the results from *Feng et al.* [2010a]. For the VIMT (Figure 12e), the moisture has been brought to the northern part of China from western North Pacific, which is in accordance with the regression result of negative EM index. In the case of CE El Niño events, significant "− +" anomalies of zonal winds at 200 hPa are located over the northern and southern part of EAWJ core (Figure 12b). This favors the southward movement of the EAWJ and increases precipitation over southern part. Enhancement of WPSH brings plentiful moisture to southern China from South China Sea (Figure 12f). These circulations tend to induce positive rainfall anomalies in the southern regions but negative anomalies in the northern part. Overall, in response to EM La Niña (pre-1991 epoch) and CE El Niño (post-1991 epoch), circulations as winds and water vapor favor the seesaw-like rainfall pattern. However, in the EM El Niño (pre-1991 epoch) and CE La Niña (post-1991 epoch), no significant circulations have been found in the compositions (figure not shown), especially for the EAWJ and water vapor.

[27] In this study, we find the Meiyu anomalies have a significant decadal shift around 1991 and are associated with EM (negative phase) and CE (positive phase) during different periods only based on diagnostic analysis. The related numerical simulation and dynamical analysis should be carried out in the future.

[28] **Acknowledgments.** We thank the Editor and three anonymous reviewers for their valuable comments and suggestions. This study is jointly sponsored by National Natural Science Foundation of China (grant 41105044), the National Basic Research Program of China (973 Program; grant 2012CB955901), National Natural Science Foundation of China (grants 51190090, 41205038), and the National Basic Research Program of China (973 Program; grant 2011CB952002).

References

Akiyama, T. (1975), Southerly transversal moisture flux into the extremely heavy rainfall zone in the Baiu season, *J. Meteorol. Soc. Jpn.*, *53*, 304–316.

Ashok, K., S. K. Behera, S. A. Rao, H. Y. Weng, and T. Yamagada (2007), El Niño Modoki and its possible teleconnection, *Geophys. Res. Lett.*, *112*, C11007, doi:10.1029/2006JC003798.

Behera, S. K., and T. Yamagata (2003), Influence of the Indian Ocean dipole on the Southern Oscillation, *J. Meteorolo. Soc. Jpn.*, *81*, 169–177.

Cai, W., P. van Rensch, T. Cowan, and A. Sullivan (2010), Asymmetry in ENSO teleconnection with regional rainfall, its multidecadal variability, and impact, *J. Climate*, *23*, 4944–4955.

Chen, W., J. Feng, and R. Wu (2013), Roles of ENSO and PDO in the link of the East Asian winter monsoon to the following summer monsoon, *J. Climate*, *26*, 622–635.

Ding, Y. H. (1992), Summer monsoon rainfalls in China, *J. Meteorol. Soc. Jpn.*, *70*, 373–396.

Ding, Y. H., Z. Y. Wang, and Y. Sun (2008), Inter-decadal variation of the summer precipitation in East China and its association with decreasing Asian summer monsoon. Part I: Observed evidences, *Int. J. Climatol.*, *28*, 1139–1161.

Du, Y., Y. C. Zhang, and Z. Q. Xie (2009), Impacts of the zonal position of the East Asian westerly jet core on precipitation distribution during Meiyu of China, *Acta Meteo. Sinica*, *23*, 506–516.

Feng, J., W. Chen, C.-Y. Tam, and W. Zhou (2010a), Different impacts of El Niño and El Niño Modoki on China rainfall in the decaying phases, *Int. J. Climatol.*, *31*(14), 2091–2101, doi:10.1005/joc.2217.

Feng, J., L. Wang, W. Chen, S. K. Fong, and K. C. Leong (2010b), Different impacts of two types of Pacific Ocean warming on Southeast Asian rainfall during boreal winter, *J. Geophys. Res.*, *115*, D24122, doi:10.1029/2010JD014761.

Gong, D. Y., and C. H. Ho (2002), Shift in the summer rainfall over the Yangtze River valley in the late 1970s, *Geophys. Res. Lett.*, *29*(10), 1436, doi:10.1029/2001GL014523.

Hartmann, B., and G. Wendler (2005), The significance of the 1976 Pacific Climate Shift in the climatology of Alaska, *J. Climate*, *18*, 4824–4839.

Hoerling, M. P., A. Kumar, and M. Zhong (1997), El Niño, La Niña, and the nonlinearity of their teleconnections, *J. Climate*, *10*, 1769–1786.

Hu, Z. Z. (1997), Interdecadal variability of summer climate over East Asia and its associated with 500 hPa height and global sea surface temperature, *J. Geophys. Res.*, *102*, 19,403–19,412.

Hu, Z. Z., S. Yang, and R. Wu (2003), Long-term climate variations in China and global warming signals, *J. Geophys. Res.*, *108*(D19), 4614, doi:10.1029/2003JD003651.

Huang, R. H., and Y. F. Wu (1989), The influence of ENSO on the summer climate change in China and its mechanism, *Adv. Atmos. Sci.*, *6*, 21–32.

Huang, G., K. M. Hu, and S. P. Xie (2010), Strengthening of Tropical Indian Ocean teleconnection to the Northwest Pacific since the mid-1970s: An atmospheric GCM study, *J. Climate*, *23*, 5294–5304.

Huang, D. Q., J. Zhu, and X. Y. Kuang (2011), Decadal variation of different durations of continuous Meiyu precipitation and the possible cause, *Chin. Sci. Bull.*, *56*, 424–431.

Huffman, G. J., D. T. Bolvin, and R. F. Adler (2011), Last updated GPCP Version 2.2 combined precipitation data set. WDC-A, NCDC, Asheville, NC (2011). Dataset accessed at http://www.ncdc.noaa.gov/oa/wmo/wdcamet-ncdc.html

Ji, L., S. Sun, and K. Arpe (1997), Model study on the interannual variability of Asian winter monsoon and its influence, *Adv. Atmos. Sci.*, *14*, 1–22.

Kajikawa, Y., and B. Wang (2012), Interdecadal change of the South China Sea summer monsoon onset, *J. Climate*, *25*, 3207–3218.

Kalnay, E., et al. (1996), The NCEP/NCAR 40-year reanalysis project, *Bull. Am. Meteorol. Soc.*, *77*, 437–472.

Karori, M. A., J. Li, and F. Jin (2013), The asymmetric influence of the two types of El Niño and La Niña on summer rainfall over Southeast China, *J. Climate*, *26*, 4567–4582.

Kug, J. S., F. F. Jin, and S. I. An (2009), Two types of El Niño events: Cold tongue El Niño and warm pool El Niño, *J. Climate*, *22*, 1499–1515.

Li, S. L., J. Lu, G. Huang, and K. M. Hu (2008), Tropical Indian Ocean basin warming and East Asian summer monsoon: A multiple AGCM study, *J. Climate*, *21*, 6080–6088.

Li, H. M., A. G. Dai, T. J. Zhou, and J. Lu (2010), Responses of East Asian summer monsoon to historical SST and atmospheric forcing during 1950–2000, *Clim. Dyn.*, *34*, 501–514.

Liang, P., and J. H. He (2008), Review for climate change of Meiyu over Yangtze-Huaihe Basins (in Chinese), *Plateau Meteorol.*, *27*(suppl), 1–15.

Ma, Y., W. Chen, S. Fong, K. Leong, and W. Leong (2012), Interannual and interdecadal variations of precipitation over eastern China during Meiyu season and their relationships with the atmospheric circulation and SST (in Chinese), *Chin. J. Atmos. Sci.*, *36*(2), 397–410.

McPhaden, M. (1999), Genesis and evolution of the 1997–1998 El Niño, *Science*, *283*, 950–954.

North, G. R., T. L. Bell, R. F. Cahalan, and F. J. Moeng (1982), Sampling errors in the estimation of empirical orthogonal functions, *Mon. Weather Rev.*, *110*, 699–706.

Picaut, J., E. Hackert, A. Busalacchi, R. Murtugudde, and G. Lagerloef (2002), Mechanisms of the 1997–1998 El Niño–La Niña, as inferred from space-based observations, *J. Geophys. Res.*, *107*(C5), 3037, doi:10.1029/2001JC000850.

Rasmusson, E. M., and T. H. Carpenter (1982), Variation in tropical sea surface temperature and surface wind fields associated with Southern Oscillation/El Niño, *Mon. Weather Rev.*, *110*, 354–384.

Rayner, N. A., D. E. Parker, E. B. Horton, C. K. Folland, L. V. Alexander, D. P. Rowell, E. C. Kent, and A. Kaplan (2003), Global analyses of sea surface temperature, sea ice, and night marine air temperature since the late nineteenth century, *J. Geophys. Res.*, *108*(D14), 4407, doi:10.1029/2002JD002670.

Ren, H. L., and F. F. Jin (2011), Niño indices for two types of ENSO, *Geophys. Res. Lett.*, *38*, L04704, doi:10.1029/2010GL046031.

Rodriguez-Fonseca, B., et al. (2010), Interannual and decadal SST-forced responses of the West African monsoon, *Atmos. Sci. Lett.*, *12*, 67–74.

Si, D., Y. H. Ding, and Y. J. Liu (2009), Decadal northward shift of the Meiyu belt and the possible cause, *Chin. Sci. Bull.*, *54*, 4742–4748.

Tao, S. Y., and L. X. Chen (1987), A review of recent research on the East Asian summer monsoon in China, *Reviews in Monsoon Meteorology*, C.-P. Chang and Krishnamurti, Eds., Oxford University Press, 60–92.

Tomita, T., and T. Yasunari (1996), Role of the northeast winter monsoon on the biennial oscillation of the ENSO/monsoon system, *J. Meteorol. Soc. Jpn.*, *74*, 399–413.

Wan, R. J., T. M. Wang, and G. X. Wu (2008), Temporal variations of the spring persistent rains and South China Sea sub-high and their correlations to the circulation and precipitation of the East Asian Summer Monsoon, *Acta Meteorol. Sinica*, *22*, 530–537.

Wang, H. (2001), The weakening of Asian monsoon circulation after the end of 1970's, *Adv. Atmos. Sci.*, *18*, 376–386.

Wang, B., R. G. Wu, and X. H. Fu (2000), Pacific–East Asian teleconnection: How does ENSO affect East Asian climate?, *J. Climate*, *13*, 1517–1536.

Weng, H., K. Ashok, S. K. Behera, A. Rao, and T. Yamagata (2007), Impacts of recent El Niño Modoki on dry/wet conditions in the Pacific rim during boreal summer, *Clim. Dyn.*, *29*, doi:10.1007/s00382-007-0234-0.

Weng, H. Y., G. Wu, Y. Liu, S. K. Behera, and T. Yamagata (2011), Anomalous summer climate in China influenced by the tropical Indo-Pacific Oceans, *Clim. Dyn.*, *36*, 769–782.

Wu, R. G., and B. Wang (2002), A contrast of the east Asian summer monsoon-ENSO relationship between 1962–77 and 1978–93, *J. Climate*, *15*, 3266–3279.

Wu, R. G., J. L. Kinter III, and B. P. Kirtman (2005), Discrepancy of interdecadal changes in the Asian region among the NCEP-NCAR reanalysis, objective analyses, and observations, *J. Climate*, *18*, 3048–3067.

Wu, B., T. J. Zhou, and T. Li (2009), Seasonally evolving dominant interannual variability modes of East Asian climate, *J. Climate*, *22*, 2992–3005.

Wu, B., T. Li, and T. J. Zhou (2010a), Relative contributions of the Indian Ocean and local SST anomalies to the maintenance of the western North Pacific anomalous anticyclone during El Niño decaying summer, *J. Climate*, *23*, 2974–2986.

Wu, B., T. Li, and T. J. Zhou (2010b), Asymmetry of atmospheric circulations over the Western North Pacific between El Niño and La Niña, *J. Climate*, *23*, 4807–4822.

Xie, S. P., K. M. Hu, J. Hafner, H. Yokinaga, Y. Du, G. Huang, and T. Sampe (2009), Indian Ocean capacitor effect on Indo-western Pacific climate during the summer following El Niño, *J. Climate*, *22*, 730–747.

Xie, S. P., Y. Du, G. Huang, X. T. Zheng, H. Tokinaga, K. Hu, and Q. Liu (2010), Decadal shift in El Niño influences on Indo-western Pacific and East Asian climate in the 1970s, *J. Climate*, *23*, 3352–3368.

Xin, X., R. Yu, T. Zhou, and B. Wang (2006), Drought in late spring of South China in recent decades, *J. Climate*, *19*, 3197–3206.

Xu, Q. (2001), Abrupt change of the mid-summer climate in central east China by the influence of atmospheric pollution, *Atmos. Environ.*, *35*, 5029–5040.

Yang, J. L., Q. Y. Liu, S. P. Xie, Z. Y. Liu, and L. X. Wu (2007), Impact of the Indian Ocean SST basin mode on the Asian summer monsoon, *Geophys. Res. Lett.*, *34*, L02708, doi:10.1029/2006GL028571.

Ye, H., and R. Y. Lu (2011), Subseasonal variation in ENSO-related East Asian rainfall anomalies during summer and its role in weakening the relationship between the ENSO and summer rainfall in eastern China since the late 1970s, *J. Climate*, *24*, 2271–2284.

Yeh, S. W., J. S. Kug, B. Dewitte, M. H. Kwon, B. P. Kirtman, and F. F. Jin (2009), El Niño in a changing climate, *Nature*, *461*, 511–514, doi:10.1038/nature08316.

Yim, S. Y., J. G. Jhun, and S. W. Yeh (2008), Decadal change in the relationship between east Asian-western North Pacific summer monsoon and ENSO in the mid-1990s, *Geophys. Res. Lett.*, *35*, L20711, doi:10.1029/2008GL035751.

Yim, S. Y., B. Wang, and M. Kwon (2013), Interdecadal change of the controlling mechanisms for East Asian early summer rainfall variation around the mid-1990s, *Clim. Dyn.*, doi:10.1007/s00382-013-1760-6.

Yu, R. C., and T. J. Zhou (2007), Seasonality and three-dimensional structure of interdecadal change in the East Asian monsoon, *J. Climate*, *20*, 5344–5355.

Yu, R. C., B. Wang, and T. J. Zhou (2004), Tropospheric cooling and summer monsoon weakening trend over East Asia, *Geophys. Res. Lett.*, *31*, L22212, doi:10.1029/2004GL021270.

Yuan, Y., H. Yang, and C. Y. Li (2012), Study of El Niño events of different types and their potential impact on the following summer precipitation in China (in Chinese), *Acta Meteorol. Sinica*, *70*, 467–478.

Zhang, R. H., A. Sumi, and M. Kimoto (1996), Impact of El Niño on the East Asian monsoon: A diagnostic study of the ’86/87 and ’91/92 events, *J. Meteorol. Soc. Jpn.*, *74*, 49–62.

Zhang, Y. C., X. Y. Kuang, W. D. Guo, and T. J. Zhou (2006), Seasonal evolution of the upper-tropospheric westerly jet core over East Asia, *Geophys. Res. Lett.*, *33*, L11708, doi:10.1029/2006GL026377.

Zhao, Y., and Y. F. Qian (2009), Analyses of the impacts of global SSTA on precipitation anomaly in China (in Chinese), *J. Trop. Meteorol.*, *25*, 561–570.

Zhou, L. T. (2011), Interdecadal change in sea surface temperature anomalies associated with winter rainfall over South China, *J. Geophys. Res.*, *116*, D11101, doi:10.1029/2010JD015425.

Zhou, L. T., and R. H. Huang (2010), Interdecadal variability of summer rainfall in northwest China and its possible causes, *Int. J. Climatol.*, *30*, 549–557.

Zhou, T. J., and R. C. Yu (2005), Atmospheric water vapor transport associated with typical anomalous summer rainfall patterns in China, *J. Geophys. Res.*, *110*, D08104, doi:10.1029/2004JD005413.

Zhou, T., D. Gong, J. Li, and B. Li (2009a), Detecting and understanding the multi-decadal variability of the East Asian Summer Monsoon—Recent progress and state of affairs, *Meteorol. Z.*, *18*, 455–467.

Zhou, T. J., et al. (2009b), Why the Western Pacific Subtropical High has extended westward since the late 1970s, *J. Climate*, *22*, 2199–2214.

Zhu, J., D. Q. Huang, Y. F. Qian, and H. J. Lin (2010), Uneven characteristics of warm extremes during Meiyu period over Yangtze-Huaihe region and its configuration with circulation systems (in Chinese), *Chin. J. Geophys.*, *53*, 2310–2320.